

STEADY-STATE DEFORMATION OF SOME LITHIUM CERAMICS*

R. B. Poeppel, J. L. Routbort,[†] M. C. Billone,
D. S. Applegate, E. Buchmann, and B. Lonschien

Materials and Components Technology Division
Materials Science Division
Argonne National Laboratory
Argonne, Illinois 60439

May 1987

CONF-8704230--1

DE88 003116

The submitted manuscript has been authored by a contractor of the U. S. Government under contract No. W-31-109-ENG-38. Accordingly, the U. S. Government retains a nonexclusive, royalty-free license to publish or reproduce the published form of this contribution, or allow others to do so, for U. S. Government purposes.

DISCLAIMER

This report was prepared as an account of work sponsored by an agency of the United States Government. Neither the United States Government nor any agency thereof, nor any of their employees, makes any warranty, express or implied, or assumes any legal liability or responsibility for the accuracy, completeness, or usefulness of any information, apparatus, product, or process disclosed, or represents that its use would not infringe privately owned rights. Reference herein to any specific commercial product, process, or service by trade name, trademark, manufacturer, or otherwise does not necessarily constitute or imply its endorsement, recommendation, or favoring by the United States Government or any agency thereof. The views and opinions of authors expressed herein do not necessarily state or reflect those of the United States Government or any agency thereof.

Presented at the Symposium on "Fabrication and Properties of Lithium Ceramics" at the 89th Annual Meeting of the American Ceramic Society, April 26-30, 1987, Pittsburgh, PA.

*Work supported by the U. S. Department of Energy, Office of Fusion Energy, under Contract W-31-109-Eng-38.

MASTER

DISTRIBUTION OF THIS DOCUMENT IS UNLIMITED

STEADY-STATE DEFORMATION OF SOME LITHIUM CERAMICS

R. B. Poeppel, J. L. Routbort,[†] M. C. Billone,
D. S. Applegate, E. Buchmann, and B. Lonschien

Materials and Components Technology Division
[†]Materials Science Division
Argonne National Laboratory
Argonne, Illinois 60439

ABSTRACT

The stress-strain behavior of Li_2O , LiAlO_2 , and Li_2ZrO_3 polycrystals, with densities varying from 0.70 to 0.95 of the theoretical, has been measured in constant-crosshead-speed compression tests at temperatures of 700–1000°C with strain rates ranging from about 10^{-6} to 10^{-4} s^{-1} . A steady-state stress, σ_s , for which the work-hardening rate becomes zero, was achieved. These results, therefore, yield information equivalent to that obtained from creep experiments. Limited data on LiAlO_2 and Li_2ZrO_3 were obtained. Nevertheless, under comparable conditions the lithium aluminate and zirconate were considerably stronger than the Li_2O . This finding may be related to differences in crystal structure. It is, however, likely that in operation as a fusion breeder blanket material, the oxide will swell whereas the aluminate and the zirconate will crack.

INTRODUCTION

A number of lithium-bearing ceramics (e.g., Li_2O , LiAlO_2 , Li_4SiO_4 , and Li_2ZrO_3) are candidate tritium-breeding materials for the blanket region of proposed fusion reactors. While a great deal of effort has been focused on the thermal and tritium transport properties of these materials, relatively little work has been done to determine the mechanical properties of these ceramics. Although the breeder ceramic does not serve a structural purpose in

the blanket, two design issues require knowledge of mechanical properties of the breeder ceramic. With differential (i.e., ceramic vs structural alloy) thermal expansion and helium-induced swelling as a driving force, breeder-structure mechanical interaction (BSMI) could limit the lifetime of the blanket. Also, differential thermal expansion and swelling within the breeder ceramic itself could induce stresses severe enough to crack the ceramic. Such cracks may cause hot spots in the breeder by increasing the resistance to heat flow. Characterization of the elastic, creep, and fracture-toughness properties of breeder ceramics is desirable in order to allow resolution of these design issues.

In previous publications,^{1,2} the elastic and steady-state thermal creep properties of Li_2O were reported. Compressive, constant-strain-rate tests were used to determine the creep rates of porous, polycrystalline Li_2O in the temperature range of 700 to 950°C. The purpose of this present work is to gain comparable knowledge of creep rates in LiAlO_2 and Li_2ZrO_3 . While such a scoping effort does not lead to full characterization of the creep relationship for these materials, it does allow for qualitative and semiquantitative comparisons to be made.

EXPERIMENTAL PROCEDURES

The compressive creep tests were performed on sintered right circular cylinders approximately 5 mm in diameter by 10 mm long loaded along the axial direction.

(1) Sample Preparation

Lithium aluminate and lithium zirconate were prepared by reacting stoichiometric mixtures of lithium carbonate with alumina and zirconia, respectively, in air for ~72 h at 650°C. The resulting products were mixed in

a 70% isopropyl alcohol-30% water solution containing a polyethylene glycol binder with a nominal molecular weight of 3350. The amount of binder used was 2% by weight of the ceramic powder. A small amount of plasticizer (~0.5 wt %) was included. After ball milling, these mixtures were dried in a laboratory spray dryer. The samples were pressed in a steel die at pressures between 90 and 190 N/mm² and fired in air to about ~1000°C.

(2) Mechanical Testing

The stress-strain behavior of the pellets whose faces were ground flat and parallel using 15 μm diamond paste was measured in compression using an apparatus that has already been described.^{3,4} Specimens were tested in flowing argon using alumina tooling separated from the sample by a thin sheet of Pt to prevent interdiffusion. Test data were recorded as load vs time. Final specimen dimensions were used to convert the load/time data to stress vs strain. Tests were performed using a constant crosshead velocity which was converted to strain rate, $\dot{\epsilon}$, by dividing by the initial length. Total strain never exceeded 5% and therefore, $\dot{\epsilon}$ was constant to within 5%. Some specimens were intentionally fractured at room temperature after testing and examined with a scanning electron microscope. The grains in a LiAlO₂ sample deformed at 1000°C grew from an initial size of about 0.5 μm to 10 μm while the grain size of the Li₂ZrO₃ samples remained approximately unchanged from the initial 1/4 μm size. SEM micrographs are shown in Figs. 1 (LiAlO₂) and 2 (Li₂ZrO₃).

EXPERIMENTAL RESULTS

A stress vs strain plot obtained for a 72% TD LiAlO₂ sample deformed at 800°C with $\dot{\epsilon} = 5 \times 10^{-6} \text{ s}^{-1}$ is shown in Fig. 3. A steady-state stress, σ_s , defined as the stress at which the work-hardening rate ($d\sigma/d\epsilon$) equals zero is not achieved. However, an estimate of the steady-state stress can be made by

the intercept of the $d\sigma/d\epsilon$ vs σ plot at $d\sigma/d\epsilon = 0$.³ The extrapolated value of σ_s obtained for the data shown in Fig. 3 is 167 MPa. It was not possible to plastically deform the high-density, larger diameter LiAlO_2 samples because of limitations on the size of applied load dictated by the tooling. For these samples, only a lower bound can be placed on the value of σ_s . The data for LiAlO_2 are presented in Table I. Representative values for Li_2O are also shown for comparison.²

A direct measurement of the steady-state stress was possible for Li_2ZrO_3 as indicated in Fig. 4 which is a stress vs strain plot for an 87% TD sample deformed at 900°C at three strain rates. The data for the 87% TD zirconate are compared to that of lithium oxide in Fig. 5 which is a log-log plot of $\dot{\epsilon}$ vs σ_s .

DISCUSSION

The most important observation from this investigation is that in all tests, both the lithium zirconate and the lithium aluminate are considerably stronger than Li_2O . Differences in density, as well as $\dot{\epsilon}$ and test temperature preclude an exact comparison of the data for LiAlO_2 and Li_2O presented in Table I. The grain sizes of the aluminate and Li_2O were comparable. However, it has been shown that the steady-state stress in lithium oxide is a function of porosity, decreasing with increasing porosity, P , as $\exp(-2.7P)$.² If one applies this correction to the 72% TD test at 800°C , $\sigma_s \approx 200$ MPa, which is 8 times larger than the corresponding value of 25 obtained for 90% TD Li_2O at 800°C .

The data in Fig. 5, which is a comparison of the results for Li_2O and the 87% TD Li_2ZrO_3 , also indicated that the lithium zirconate is considerably stronger than the lithium oxide. In this case, the test temperatures, $\dot{\epsilon}$, and

densities are comparable, but the $1/4 \mu\text{m}$ grain size of the zirconate is considerably smaller than the smallest grain size Li_2O tested. While the steady-state stress of Li_2O was independent of grain size in the range of 12 to $75 \mu\text{m}$, it is not safe to assume that the independence could be extended to the very small grain sizes of the zirconate. Therefore, some or all of the strengthening effect may be the smaller grain size via a Hall-Petch relationship. Additional experimental evidence would be needed to verify this point.

Nevertheless, this result is consistent with simple theoretical considerations. It was shown that deformation in Li_2O was controlled by dislocation motion.² The stress exponent for the lithium zirconate obtained from Fig. 5 is greater than 1. It is very likely, therefore, that dislocation motion controls deformation in the zirconate as well. The elastic energy of a dislocation is proportional to Gb^2 , where G is the shear modulus and b is the Burger's vector. The tetragonal crystal structure of both the LiAlO_2 and the Li_2ZrO_3 results in much larger values of b than is the case of the simple antiferroite Li_2O . Furthermore, the room-temperature shear modulus of LiAlO_2 is three times larger than that of comparable density Li_2O .^{1,5} We are unaware of any modulus data for the zirconate, but it should be comparable to that of the aluminate. Therefore, because both G and b are larger in the aluminate and zirconate than in Li_2O , it may be expected that the latter materials are more difficult to deform, as was observed.

The creep experiments of Rasneur⁵ performed at 700°C on $0.4 \mu\text{m}$ grain size LiAlO_2 constitute the only other mechanical property measurement on either the aluminate or the zirconate. These measurements were performed at 50, 80, and 100 MPa and resulted in strain rates of 10^{-11} to 10^{-8} s^{-1} . These data, when extrapolated by 10^3 to our strain rates, compare very well (Fig. 6). The

extrapolated stress at $\dot{\epsilon} = 5 \times 10^{-6} \text{ s}^{-1}$ from the creep data is about 205 MPa, while the measured value at 800°C is 167 MPa. Compensation for the lower temperature by a reasonable activation energy would increase the measured value. No SEM was performed on the LiAlO_2 sample deformed at 800°C, but it is reasonable to assume that at this temperature there was little grain growth; therefore, the grain sizes of the samples of the two studies were comparable.

There is another interesting aspect of the deformation of the lithium zirconate that should be explored. The data obtained at 900°C indicate that the stress exponent decreases to as low as 1.3 at low stresses. A similar decrease in stress exponent was observed for Li_2O and attributed to the onset of viscous flow.²

It is clear that the analysis of these results do not yield a complete understanding of the mechanical properties of the lithium aluminate or zirconate. The deformation mechanisms can only be elucidated by extensive, careful experiments performed on well-characterized specimens. Nevertheless, the results reported here can have a significant impact on the choice of a breeder-blanket material.

From a modeling and performance prediction viewpoint, it is interesting to note that Li_2O has the highest thermal expansion coefficient and helium-induced swelling rate, as well as the highest creep (and probably hot pressing) rate, of the three materials studied. Therefore, while contact between Li_2O and the structural metal may occur in most designs, interface pressures due to BSMI may be relaxed to tolerable levels due to the "softness" of the porous Li_2O . In contrast, the two materials studied in this current effort have lower expansion coefficients and helium-induced swelling rates as compared to Li_2O , but appear to be more creep resistant. Thus, while the driving mechanisms for thermal stress cracking and BSMI are less for LiAlO_2

and Li_2ZrO_3 as compared to Li_2O , the stress relaxation mechanisms due to creep and hot pressing are also probably less. Clearly, more data are required for these materials in order to assess quantitatively the findings of these studies.

SUMMARY

Rather incomplete deformation data have been obtained for lithium aluminate, LiAlO_2 , and lithium zirconate, Li_2ZrO_3 , at temperatures between 800 and 1000°C and for strain rates between 1×10^{-6} and $1 \times 10^{-5} \text{ s}^{-1}$. These two materials appear much more creep resistant than another candidate breeder blanket material, Li_2O . The reason for the increased creep resistance is probably the result of more complex crystal structures. The significance of these data to breeder blanket design is that stress-induced cracking is more likely in lithium aluminate and lithium zirconate and that mechanical interaction between the breeder material and structural components more severe as compared with lithium oxide, a breeder material with a much lower creep resistance.

ACKNOWLEDGMENT

The work was supported by the U. S. Department of Energy, Office of Fusion Energy, under Contract W-31-109-Eng-38.

REFERENCES

1. M. C. Billone, Y. Y. Liu, R. B. Poeppe1, J. L. Routbort, K. C. Goretta, and D. S. Kupperman, *J. Nucl. Mater.* 141-143, 282 (1986).
2. K. C. Goretta, D. S. Applegate, R. B. Poeppe1, M. C. Billone, and J. L. Routbort, *J. Nucl. Mater.* 148, 166 (1987).

3. J. L. Routbort, Acta Met. 27, 649 (1979).
4. J. L. Routbort, Acta Met. 30, 663 (1982).
5. B. Rasneur, Fusion Tech. 8, 1909 (1985).

Table I. Comparison of Steady-State Stress of LiAlO₂ and Li₂O

Deformation Temp. (°C)	Fraction of Theoretical Density (%)	Strain Rate (s ⁻¹)	Steady-State Stress (MPa)
<u>LiAlO₂</u>			
800	72	5 x 10 ⁻⁶	167 ^a
1000	95	5 x 10 ⁻⁶	>262
1000	99	2 x 10 ⁻⁶	335 ^a
<u>Li₂O</u>			
800	90	2 x 10 ⁻⁶	25
900	90	2 x 10 ⁻⁶	15

^aExtrapolated.



Fig. 1. Comparison of the microstructure of lithium aluminate before and after testing. (a) As-fabricated, magnification 5000X, and (b) after deformation at 1000°C, magnification 1000X.

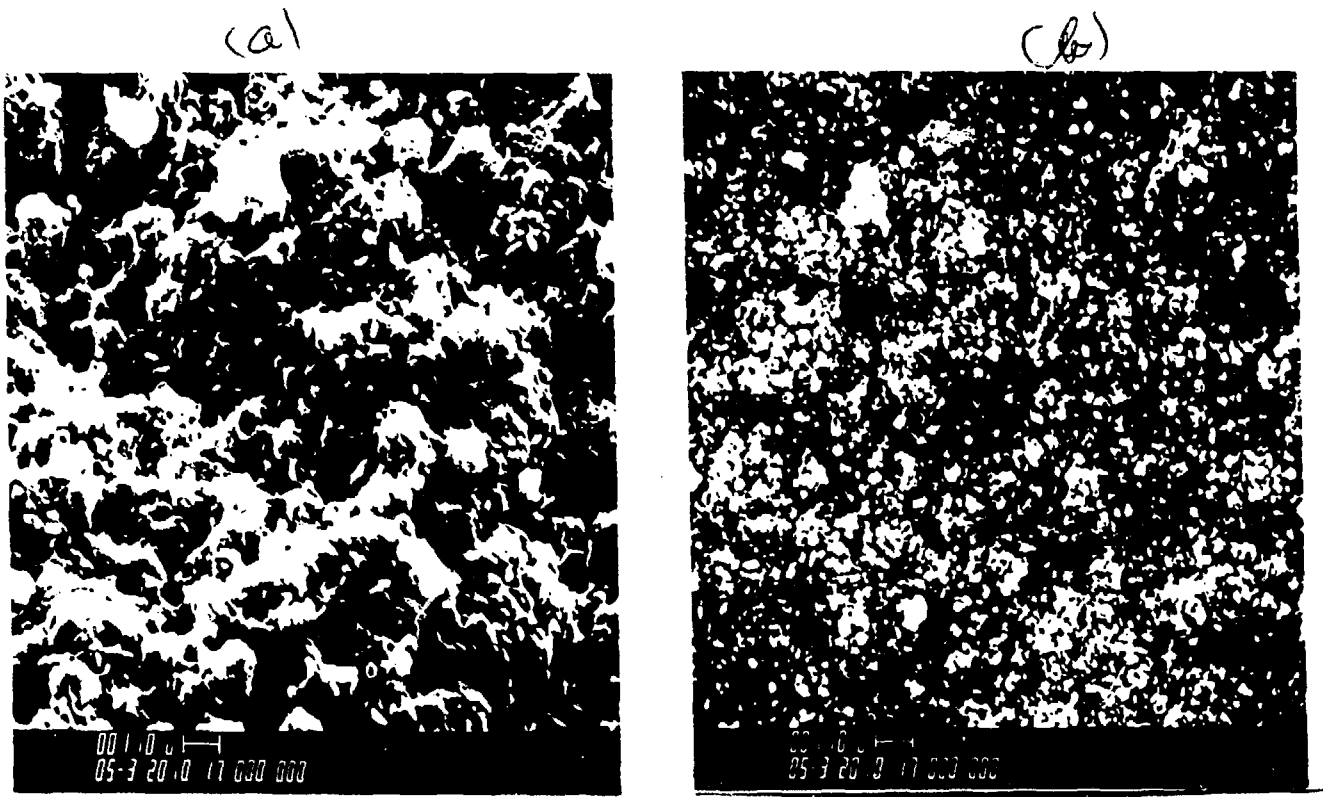


Fig. 2. Comparison of the microstructure of lithium zirconate before and after testing. Magnification 5000X. (a) As fabricated and (b) after deformation at 900°C.

DEFORMATION BEHAVIOR

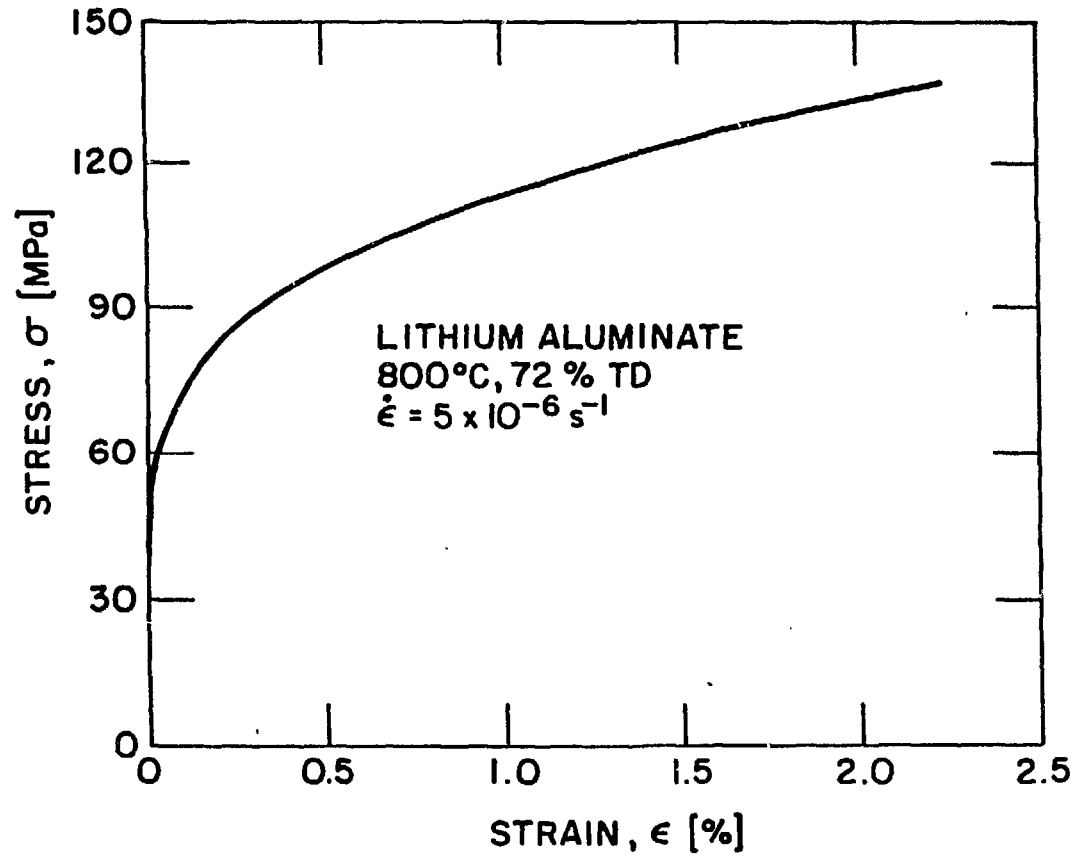


Fig. 3. Deformation behavior of lithium aluminate at 800°C.

DEFORMATION BEHAVIOR

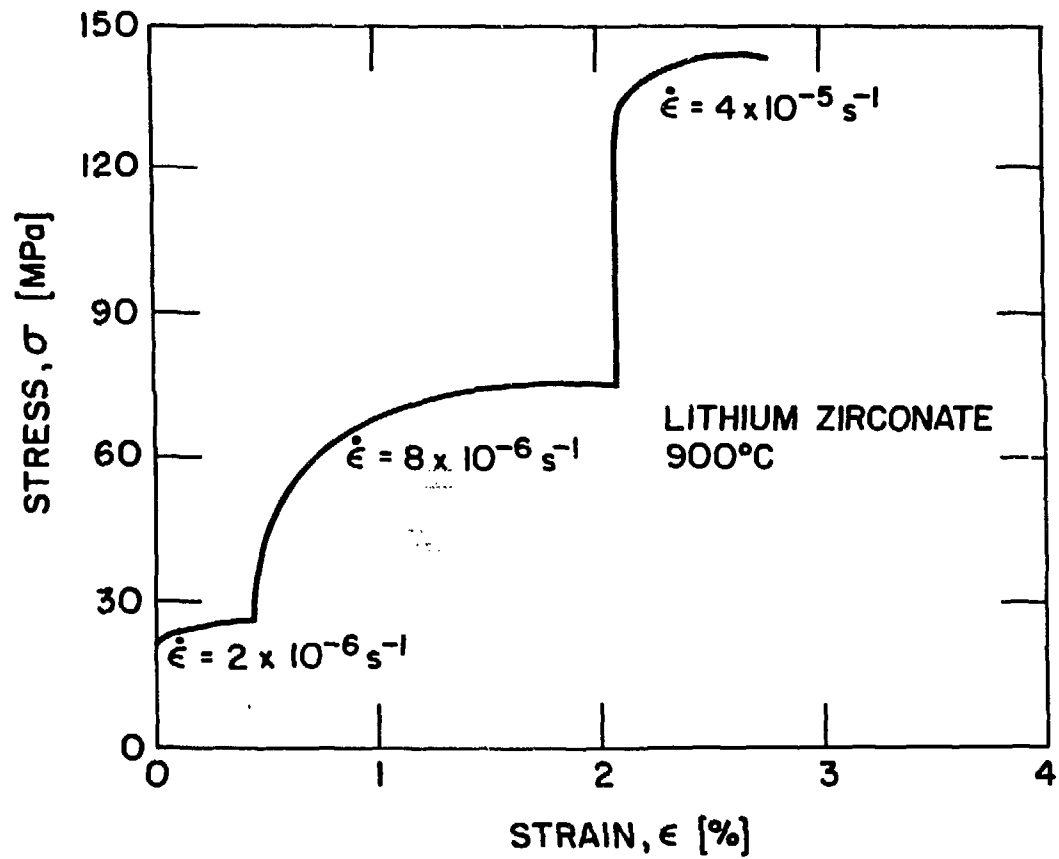


Fig. 4. Deformation behavior of lithium zirconate at 900°C.

STEADY-STATE DEFORMATION

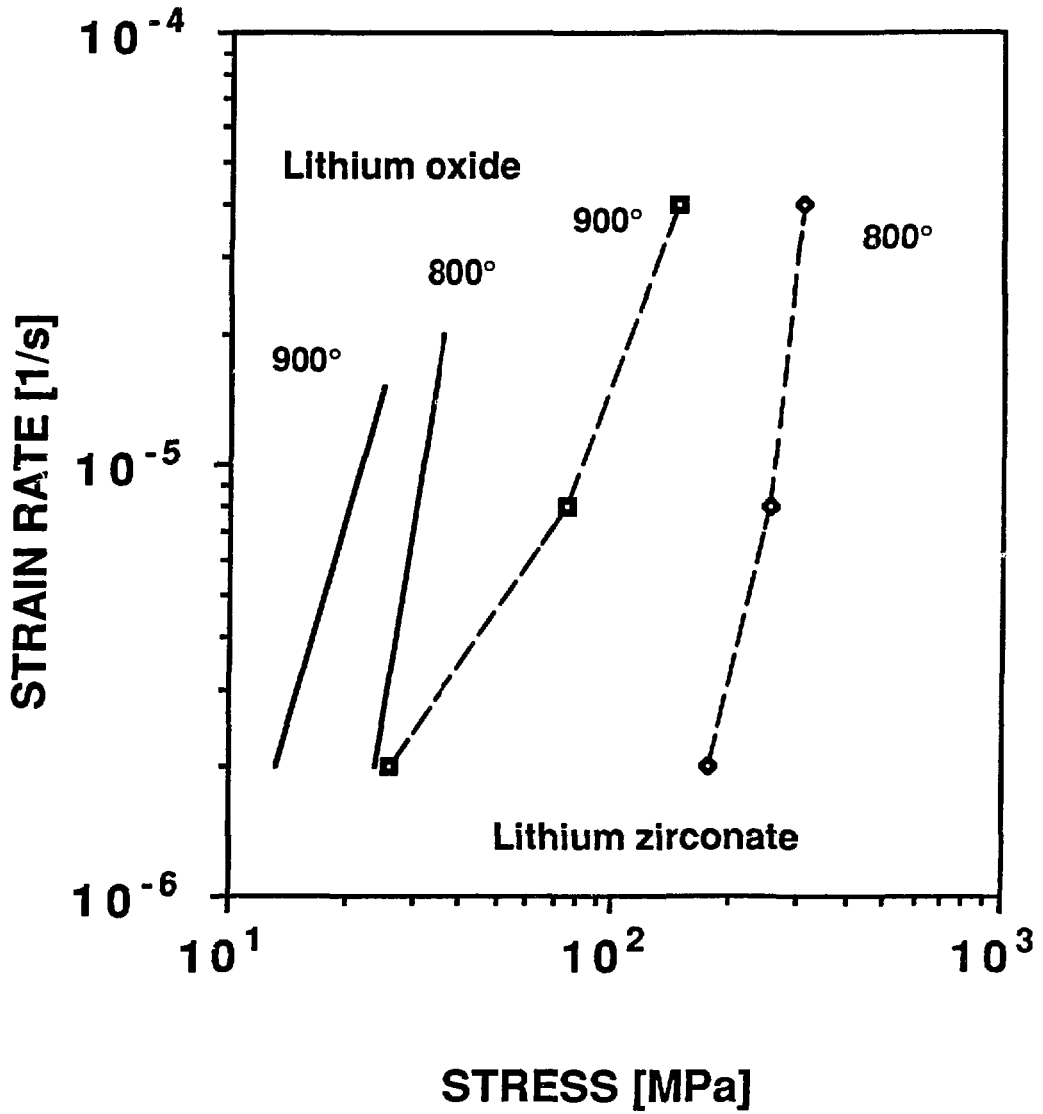


Fig. 5. Comparison of the steady-state stress-strain rate behavior of lithium zirconate and lithium oxide at 800 and 900°C.

DEFORMATION BEHAVIOR

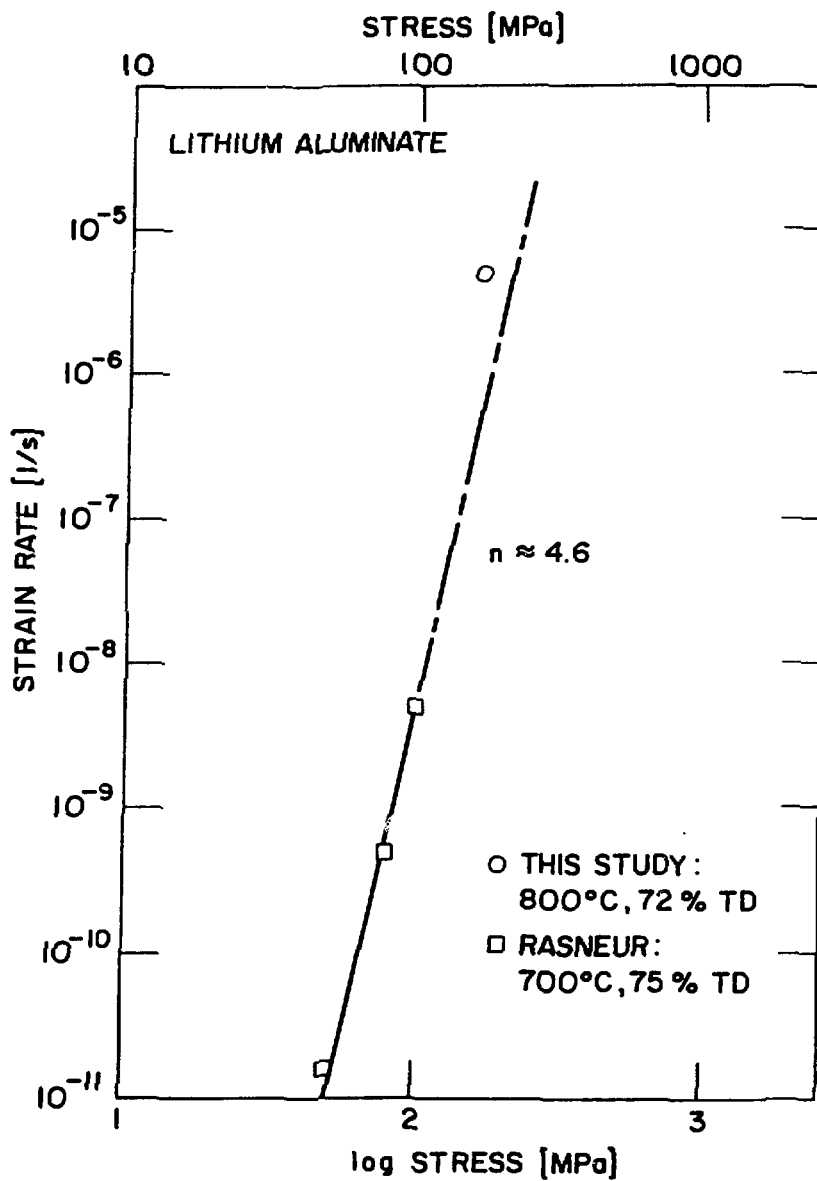


Fig. 6. Comparison of the deformation behaviors at low strain rates (Rasneur⁵) and high strain rate (this study).